

Freestanding nanostructures for three-dimensional superconducting nanodevices

Ajuan Cui, Wuxia Li, Qiang Luo, Zhe Liu, and Changzhi Gu

Citation: [Applied Physics Letters](#) **100**, 143106 (2012); doi: 10.1063/1.3701283

View online: <http://dx.doi.org/10.1063/1.3701283>

View Table of Contents: <http://scitation.aip.org/content/aip/journal/apl/100/14?ver=pdfcov>

Published by the [AIP Publishing](#)

Articles you may be interested in

[Three-dimensional nanoscale superconducting quantum interference device pickup loops](#)

Appl. Phys. Lett. **97**, 222506 (2010); 10.1063/1.3521262

[Evaluations of the hopping growth characteristics on three-dimensional nanostructure fabrication using focused ion beam](#)

J. Vac. Sci. Technol. B **27**, 2698 (2009); 10.1116/1.3250240

[Fabrication of three-dimensional nanostructures by focused ion beam milling](#)

J. Vac. Sci. Technol. B **26**, 973 (2008); 10.1116/1.2912079

[Observation and characteristics of mechanical vibration in three-dimensional nanostructures and pillars grown by focused ion beam chemical vapor deposition](#)

J. Vac. Sci. Technol. B **19**, 2834 (2001); 10.1116/1.1417545

[Three-dimensional nanostructure fabrication by focused-ion-beam chemical vapor deposition](#)

J. Vac. Sci. Technol. B **18**, 3181 (2000); 10.1116/1.1319689

An advertisement for Keysight B2980A Series Picoammeters/Electrometers. The ad features a red and white color scheme with a ruler graphic at the top. The text reads: 'Confidently measure down to 0.01 fA and up to 10 PΩ'. Below this, it says 'Keysight B2980A Series Picoammeters/Electrometers' and 'View video demo >'. On the right side, there is an image of the device and the Keysight Technologies logo.

Freestanding nanostructures for three-dimensional superconducting nanodevices

Ajuan Cui,^{a)} Wuxia Li,^{b)} Qiang Luo, Zhe Liu, and Changzhi Gu^{b)}

Beijing National Laboratory for Condensed Matter Physics, Institute of Physics, Chinese Academy of Sciences, Beijing 100190, China

(Received 25 October 2011; accepted 20 March 2012; published online 4 April 2012)

Free-space nanostructures are the fundamental building blocks of three-dimensional (3D) nanodevices with multi-functionality beyond that achievable by planar devices. Here we developed a reliable technique for the site-specific post-growth geometrical manipulation of freestanding superconducting nanowires using ion-beam irradiation with nanometer-scale resolution to fabricate uniformly shaped and sized clean-surface 3D nanostructures. Such structures could integrate with conventional superconducting quantum interference devices to detect magnetic fields both parallel and normal to the substrate. Property characterizations suggest that our focused-ion-beam technique allows tailoring of freestanding superconducting loops for size and geometry, potentially for lab-on-chip experiments. © 2012 American Institute of Physics. [<http://dx.doi.org/10.1063/1.3701283>]

Three-dimensional (3D) nanostructures and nanodevices have attracted tremendous interest in the past few years due to their excellent mechanical and physical properties. Optoelectronic devices,¹ nanosensors,² biological information detectors,³ plasmonics,⁴ and quantum devices^{5,6} based on 3D nanostructures have excellent functional properties that planar nanodevices cannot achieve. Among them, 3D superconducting quantum interference devices (SQUIDs), which can be formed by the integration of free-space multiple pick-up loops with conventional SQUID, potentially could overcome the present planar SQUID limitation of only being able to detect the field perpendicular to the substrate. It has been demonstrated that with the 3D pick-up loops, nano-SQUIDs can be used to detect different field components (B_x , B_y , and B_z) or field gradients ($\partial B_i/\partial j$), where $i, j = \{x, y, z\}$ in free-space; however, to achieve single-spin resolution, nanoscale 3D pick-up loops with uniform size and clean surface are essential.⁵ Thus, it is of great importance that we seek to explore a technique that can be used to fabricate high-quality superconducting 3D pick-up loops with quantized properties.

Direct deposition of 3D tungsten nanostructures with a slowly moving ion beam has been previously reported.^{5,7} However, the disadvantages of this technique include: (i) it requires sophisticated software packages and an expensive sample stage; (ii) it is time consuming to the point that structures can only be formed one-by-one, and intensive experimentation is required beforehand for optimized growth conditions; (iii) residual deposition underneath the suspended portion cannot be avoided, which could induce an extra conduction path and ruin the designed device functionality; (iv) it is very difficult to obtain 3D structures that are uniform in size due to the stray dose and the beam-matter interactions during the growth process. Other reported studies so far involving focused-ion-beam (FIB)-induced direct-

writing include the fabrication of C,⁸ SiO₂,⁹ and Pt¹⁰ 3D nanostructures using a slowly moving beam or a tilt stage. The disadvantages of using a tilt stage include that such method permits only very simple structures to be obtained; it lacks controllability, flexibility, efficiency, and repeatability; and it is not easy to make a solid contact between two wires to avoid residual deposition.¹⁰

In this work, superconducting tungsten nanowires were chosen as targets for exploring a technique that can be used for post-growth shape manipulation. The advantages of using FIB-induced deposition to grow tungsten nanowires for FIB-induced shape manipulation include: (i) the electrical resistivity of the freestanding tungsten nanowires is comparable to that of nanowires laterally grown on the substrate surface,⁷ making it useful to construct 3D conducting nanodevices; (ii) the nanowires have a much-higher superconducting transition temperature ($T_c \sim 5.2$ K) than the bulk counterparts,¹¹ making them a valuable option for constructing 3D superconducting nanodevices; and (iii) FIB techniques offer the means to grow true nanoscale features site-specifically with controllable size tunability, allowing us to construct free-space nanodevices with increased flexibility and controllability.

In order to develop a technology for the controllable shape manipulation of tungsten nanowires, we systematically investigated the general bending effect, including the influence of the ion beam current and the ion incident angle. 3D superconducting nanostructures were formed along with temperature-dependent measurements down to 1.8 K for basic electrical property probing. The results proved that post-growth manipulation by focused-ion-beam irradiation could be a potential method to fabricate 3D SQUIDs.

The tungsten nanowires used in this study were grown by FIB-induced deposition using a 1 pA ion beam current with W(CO)₆ as the gas precursor. The system used is a dual-beam FIB/scanning electron microscope (SEM) system. The ion source is a singly charged liquid gallium ion, which is placed at a 52° angle to the vertically oriented electron

^{a)}E-mail: cuiajuan@aphy.iphy.ac.cn.

^{b)}Authors to whom correspondence should be addressed. Electronic addresses: liwuxia@aphy.iphy.ac.cn and czgu@aphy.iphy.ac.cn.

beam column. For nanowire deposition, first, the gas precursor molecules were introduced to the substrate surface through a gas nozzle, and then an FIB with a nominal diameter of 7 nm was kept stationary in a particular position; this beam-scanning strategy was called spot-mode. The background pressure was about 5.5×10^{-5} to 1.0×10^{-6} mbar during deposition.

To explore the general bending phenomena, vertical nanowires with various heights were grown on SiO₂/Si substrates. Ion beam currents in the range of 30–100 pA with an ion energy of 30 keV were recorded. One ion beam sweep loop took 163 s under magnification of 15 000 \times , corresponding to a total area of $20.237 \times 17.470 \mu\text{m}^2$. Thus, the dwell time during scanning is 1.81×10^{-4} s, and the beam step size is 19.8 nm. Successive repeat scanning, different incident angles, and ion beam current were employed to study the bending and alignment phenomena of nanowires. After each irradiation scan, the stage was tilted to 45° off-normal to the electron beam for measuring bending by *in situ* SEM. Pairs and groups of nanowires with different sizes and interspacing were also deposited for free-space nanogap/joint-contact fabrication. For this purpose, we utilized two experimental setups: (i) irradiating the whole field of view by raster scanning or (ii) scanning a selected nanopillar or part of it by reduced raster scanning. The electrical properties of the resulting tungsten nanostructures were measured using a quantum design physical properties measurement system (PPMS) with temperature sweeping from room temperature down to 1.8 K.

Figure 1(a) shows the SEM images of tungsten nanowires irradiated with various ion beam sweep numbers to identify their free-space movement. The definitions of the

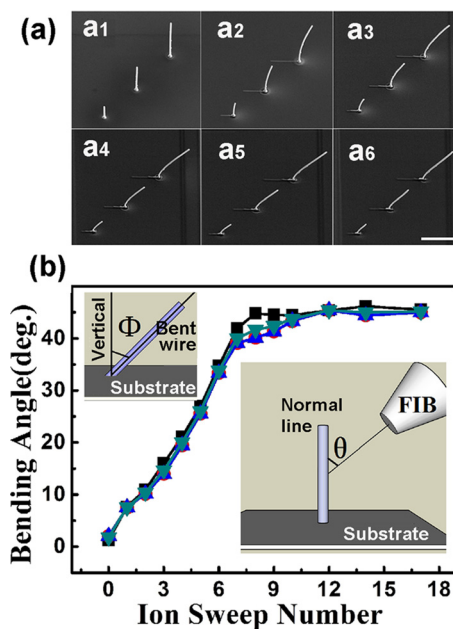


FIG. 1. (a) SEM images of the as-deposited tungsten nanowires (a1) and those irradiated with an increasing Ga ion-beam sweep number, showing the bending sequence ((a2)–(a6)). (b) The bending angle as a function of the ion sweep number. The scale bar is 2 μm . The inset in the upper left corner of (b) shows the schematic of the bending angle (Φ), and that in the lower right corner shows the definition of the ion beam incident angle (θ).

bending angle (Φ , the angle between the beginning of the wire and its angle from vertical) and of the incident direction of the irradiation ion beam (θ , the angle between the incident ion beam and the long axis of the wire) are schematically shown in the inset of Fig. 1(b). The height of the as-deposited nanowires is 1.25, 2.62, and 3.79 μm , respectively, and the radius is about 65 nm. The resultant images were taken after each ion beam scanning with a current of 100 pA and an incident angle of 40°, in the strategy of raster scanning under magnification of 15 000 \times . It can be seen from Fig. 1(a) that shorter nanowires bent more slowly; however, the time required for nanowires with different lengths to be aligned with the incident ion beam is more or less the same. Fig. 1(b) shows the bending angle as a function of the ion sweep number; it can be seen that the bending occurs toward the incident ion beam until the wires become parallel to it, and then the bending angle saturates upon further irradiation. This is similar to the observed bending of various nano-objects previously reported.^{12–17} The different colors in Fig. 1(b) stand for three different nanowires of the same length, showing that this technique has very good repeatability.

To examine the effect of the incident angle of the ion beam, three groups of nanowires with identical dimension and interspacing were used, the stage was tilted to vary the ion beam incident direction, and an ion beam current of 100 pA was scanned by raster scanning under magnification of 15 000 \times . Fig. 2(a) shows the ion beam incident angle-dependent bending of tungsten nanowires (around 2.3 μm in height and 60 nm in radius) occurring at the initial irradiation stage. Again, the pillars bent until the angle became aligned with the ion beam direction, which is 10°, 30°, and 50° with

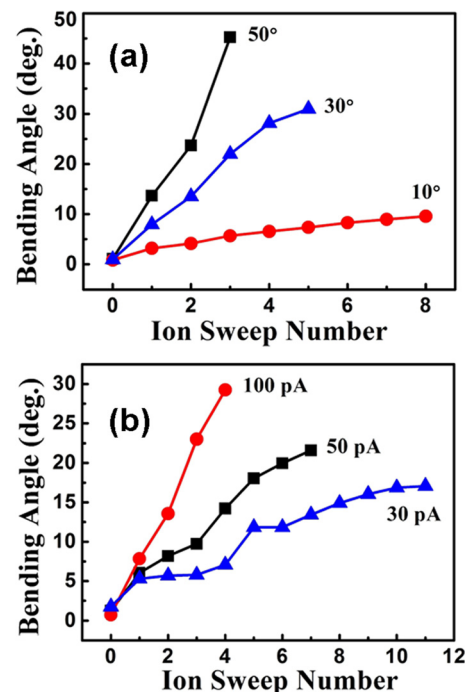


FIG. 2. The bending angle as a function of the ion sweep number for FIB-grown tungsten nanowires. (a) Bending angle for nanowires irradiated by a 100 pA ion beam with an ion beam incident angle of 50°, 30°, and 10°, respectively. (b) Bending angle for nanowires irradiated with an ion beam incident angle of 30° and an ion beam current of 100 pA, 50 pA, and 30 pA, respectively. The lines are provided to help guide the reader's eye.

respect to the vertical. Besides, it can be seen that nanowires bent faster when irradiated with a larger ion beam incident angle. The effect of the ion beam current was also explored, and the bending trend is shown in Fig. 2(b). It shows that using a higher ion beam current, it takes less time for a nanowire to achieve a higher bending angle. These findings are consistent with the results previously reported.¹⁸

Figure 3(a) shows the schematic process to construct 3D nanocontacts, multi-branched structures, and nanogaps by FIB-induced deformation. To guide the nanowire bending process and control its ultimate shape, the optimized stage-tilting angle is proposed based on the values of nanowires heights and interspacing. For instance, to form free-standing joint contact on nanowires W1 and W2 as illustrated in Fig. 3(a), where nanowire W1 should stay vertical and W2 is supposed to bend to contact with W1, the value of the proposed stage tilt angle is thus given by

$$\theta = \arctan(h_1/d). \quad (1)$$

The other condition required for solid contact formation is

$$h_2^2 \geq h_1^2 + d^2. \quad (2)$$

Here h_1 and h_2 are the heights of W1 and W2, respectively, d is the interspacing between them, and θ is the tilt angle that the stage should situate. Thus, by tilting the stage with an angle of θ , the projection length of W2 on the substrate surface is not less than d ; meanwhile, the projection length of W2 on the length direction of W1 is not less than h_1 . Fig. 3(b) shows the joint-nanocontacts formed on two rows of tungsten nanowires with heights of 2.8 and 1.5 μm and an interspacing of 2 μm ; these nanocontacts were grown on a Si substrate by FIB-induced chemical-vapor-deposition. To achieve such structures, the stage was rotated to guarantee that W1, W2, and the ion beam are aligned; reduced raster scanning was then performed to irradiate one row of nanowires by tilting the stage by 40° so that they bent toward the incident ion beam and finally made contact with the as-grown nanowires on the other row.

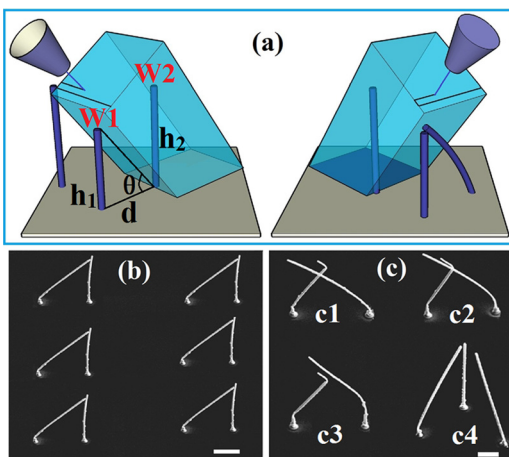


FIG. 3. Free-space tungsten nanostructures formed based on FIB-grown tungsten nanowires. (a) Schematics for the construction of joint-nanocontacts/nanogaps by the FIB-induced deformation of vertically grown nanowires. (b) SEM image of arrays of free-space joint-contacts. (c) Nanogapped and branched structures. The scale bar is 1.0 μm .

Conversely, nanogaps with a tunable distance, as can be seen from Fig. 3(c), were formed by adjusting the stage-rotation angle, the ion beam-incident angle, and the size and interspacing of the as-grown nanowires. To achieve solid contact between two wires with one of them remaining undisturbed, a reduced-raster scan is performed only to irradiate the wire to be bent. Furthermore, multi-branched structures (joined at one point) and cross-contacted/gapped structures can be formed by performing stage-rotation and stage-tilting repeatedly to manipulate the leaning direction of different wires in a combination method of irradiating a portion of a wire.

However, it is very difficult to form sophisticated nanostructures such as four-point structures with good repeatability and efficiency. In theory, the spatial precision of this technique would be determined by the resolution of the ion beam system, which is about 7 nm for the FIB we used; technically, it is also largely dependent on facility operation conditions. Nonetheless, based on the above results, we can conclude that freestanding 3D nanostructures with various geometric styles can be formed by FIB-induced deformation with reasonably good controllability, repeatability, and spatial precision.

Figure 4 shows the temperature-dependent electrical property of an air-bridge-like free-space nanostructure constructed by FIB-induced deformation (red triangles) and that for the as-grown nanowire (black circles). In the inset is a typical SEM image of free-standing 3D nanostructures. To form such a structure, first, FIB was used to deposit tungsten strips on large contact pads, which were previously formed on a SiO_2/Si substrate. Then, pairs of tungsten nanowires were deposited on the edges of the strip and one pad, followed by ion irradiation to bend one of the wires that has a higher aspect ratio (the left-side one in this case) to join the two wires. Following the method reported in our previous work,⁷ the normal state resistance and resistivity of the free-standing portion were calculated to be around 2.7 k Ω and 540 $\mu\Omega\text{ cm}$, respectively; the superconducting transition temperature derived from the curve is about of 5.1 K. For comparison, ultra-low current FIB lateral milling was used to release the as-deposited nanowire from its base for measurement of its electrical properties.¹⁹

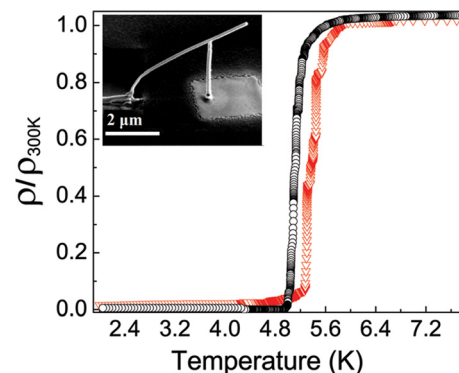


FIG. 4. The temperature-dependent normalized resistivity of a free-space tungsten nanostructure fabricated by the FIB-induced deformation of FIB-grown tungsten nanopillars (red triangle) and that of the as-deposited nanopillar without deformation (black circle). The inset shows the SEM side view image of the corresponding nanostructure.

A four-terminal-configuration was formed on the fallen nanowire, and the normalized resistivity was plotted in Fig. 4 (black), which has a slightly steeper superconducting transition since the measured structure is the nanowire itself only. The slightly broader transition width present in the free-space structures is mainly due to the tungsten strips used to connect the nanostructure to the larger contact pads. The current density is measured to be about $0.3 \times 10^4 \mu\text{A} \mu\text{m}^{-2}$. The resistivity of the vertically grown and felled W-wire is about $520 \mu\Omega \text{cm}$,⁷ and it is about $550 \mu\Omega \text{cm}$ for the as-deposited air-bridge structures.¹⁹ The resistance of the measured part is in the range of a few kilo-Ohms. Since the resistivity difference of the as-deposited, bent, and felled tungsten nanowires is less than 10%, we conclude that once a solid contact is formed, the contact resistance is negligible. Thus, we have demonstrated that the technique of focused-ion-beam irradiation can be used to form freestanding superconducting nanostructures with clean, smooth, and uniform size as well as reliable superconductivity and mechanical properties; we expect that this could be a potential method of forming super-performance superconducting nanodevices.

In conclusion, we have developed a technique for manipulating the shape and orientation of freestanding superconducting nano-objects with nanoscale resolution and accuracy by FIB-induced deformation. The deformation of the freestanding structures is highly reproducible and controllable. Free-space conducting and superconducting nanostructures were constructed, and characterization of the nanostructures' temperature-dependent electrical properties suggested that directly modifying the shape of freestanding nano-objects by ion-beam irradiation could potentially be used to fabricate versatile building blocks for free-space multifunctional nanodevices, such as one-node multi-branch 3D functional units, freestanding electrodes, wiring, and nanoswitches, especially in the construction of superconducting devices with performance that cannot be achieved by planar devices (e.g., fabrication of multiple loops in three dimensions toward the measurement of different field components or field gradients).

We would also like to point out that for ion beam current ranges from 30 to 100 pA, the bending angle is almost linearly proportional to the ion fluence (irrespective of the values of the irradiated ion beam current); however, for ion beam current as low as 1 pA, no bending was observed, and even the ion fluence is increased by using a longer exposure time. The temperature gradient and stress introduced by ion irradiation have been previously reported to explain the mechanism behind the bending of FIB-grown carbon nanopillars.¹⁸ Recently, we found that Pt wires on a SiO_2/Si substrate grown by FIB deposition bend first against and then toward

the incident ion beam, which is a different bending mechanism from those grown on conducting substrates. Factors such as electrostatic interactions between the irradiated wires, the substrate, and the impinging ions; the thermal and electrical properties of the supporting substrate and the irradiated wires; and the energy, fluence, and scanning strategy of the ion beam may all affect the bending direction and bending rate of the irradiated nanowire. However, theoretical studies and additional experiments are required in order to ascertain how to distinguish the effect from each parameter and to determine which one would dominate the whole process; we expect to conduct such research in the near future.

The authors would like to thank Dr. Paul Warburton and Dr. Jon Fenton (London Centre for Nanotechnology, UK) for very valuable discussions. This work is supported by the Outstanding Technical Talent Program of the Chinese Academy of Sciences; the National Natural Science Foundation of China under Grant Nos. 91123004, 11104334, 50825206, 10834012, and 60801043; and the National Basic Research Program (973) of China under Grant No. 2009CB930502.

- ¹J. Valentine, S. Zhang, T. Zentgraf, E. Ulin-Avila, D. A. Genov, G. Bartal, and X. Zhang, *Nature (London)* **455**, 376 (2008).
- ²P. Gouma, K. Kalyanasundaram, X. Yun, M. Stanacevic, and L. Wang, *IEEE Sens. J.* **10**, 49 (2010).
- ³B. Tian, T. Cohen-Karni, Q. Qing, X. Duan, P. Xie, and C. M. Lieber, *Science* **329**, 830 (2010).
- ⁴S. Noda, K. Tomoda, N. Yamamoto, and A. Chutinan, *Science* **289**, 604 (2000).
- ⁵E. J. Romans, E. J. Osley, L. Young, P. A. Warburton, and W. Li, *Appl. Phys. Lett.* **97**, 222506 (2010).
- ⁶T. Morita, R. Kometani, K. Watanabe, K. Kanda, Y. Haruyama, T. Hoshino, K. Kondo, T. Kaito, T. Ichihashi, J. Fujita, M. Ishida, Y. Ochiai, T. Tajima, and S. Matsui, *J. Vac. Sci. Technol. B* **21**(6), 2737 (2003).
- ⁷W. Li and P. A. Warburton, *Nanotechnology* **18**, 485305 (2007).
- ⁸S. Matsui, *Nucl. Instrum. Methods Phys. Res. B* **257**, 758 (2007).
- ⁹S. Reyntjens and R. Puers, *J. Micromech. Microeng.* **10**, 181 (2000).
- ¹⁰N. S. Rajput, M. Sarkar, A. Banerjee, N. Shukla, S. K. Tripathi, and H. C. Verma, *Micro Nano Lett.* **6**, 755 (2011).
- ¹¹E. S. Sadki, S. Ooi, and K. Hirata, *Appl. Phys. Lett.* **85**, 6206 (2004).
- ¹²L. Romano, N. G. Rudawski, M. R. Holzworth, K. S. Jones, S. G. Choi, and S. T. Picraux, *J. Appl. Phys.* **106**, 114316 (2009).
- ¹³C. Borschel, S. Spindler, D. Leroose, A. Bochmann, S. H. Christiansen, S. Nietzsche, M. Oertel, and C. Ronning, *Nanotechnology* **22**, 185307 (2011).
- ¹⁴W. J. Arora, S. Sijbrandij, L. Stern, J. Notte, H. I. Smith, and G. Barbasthis, *J. Vac. Sci. Technol. B* **25**, 2184 (2007).
- ¹⁵L. Xia, W. Wu, J. Xu, Y. Hao, and Y. Wang, *MEMS* **22**, 118 (2006).
- ¹⁶B. C. Park, K. Y. Jung, W. Y. Song, B.-H. O, and S. J. Ahn, *Adv. Mater.* **18**, 95 (2006).
- ¹⁷Z. Deng, E. Yenilmez, A. Reilein, J. Leu, H. Dai, and K. A. Moler, *Appl. Phys. Lett.* **88**, 023119 (2006).
- ¹⁸S. K. Tripathi, N. Shukla, S. Dhamodaran, and V. N. Kulkarni, *Nanotechnology* **19**, 205302 (2008).
- ¹⁹W. Li, C. Z. Gu, and P. A. Warburton, *J. Nanosci. Nanotech.* **11**, 7436 (2010).